Supplementary Materials: Pyrene-based Conjugated Polymer/Bi_2MoO_6 Z-scheme Hybrids: Facile Construction and Sustainable Enhanced Photocatalytic Performance in Ciprofloxacin and Cr(VI) Removal under Visible Light Irradiation

Xianglong Yang, Yonggang Xiang, Xuepeng Wang, Shu Li, Xing Ding and Hao Chen

1. Preparation of photocatalysts

The Bi_2MoO_6 nanobelts (1BMO) were prepared through the oleyamine-mediated hydrothermal reaction of $Bi(NO_3)_3{\cdot}5H_2O$ and $(NH_4)_6Mo_7O_{24}{\cdot}4H_2O$ [1]. The Bi_2MoO_6 microspheres (3BMO) were prepared using a solvothermal procedure. Typically, $Bi(NO_3)_3{\cdot}5H_2O$ and $Na_2MoO_4{\cdot}2H_2O$ were dissolved in the mixture solution of 7.5mL ethylene glycol (EG) and 45mL ethanol under magnetic stirring. And then the obtained clear solution was transferred into Teflon-lined stainless steel autoclave, and heated at 160 °C for 12 h. The obtained sample was isolated by washing with distilled water, dried in a vacuum oven at 80 °C for 24 h and then annealed at 350 °C in air atmosphere for 1h. Similar to the synthesis of P-2BMO, the 6.7% P-1BMO and 6.7% P-3BMO hybrids were also fabricated through the in-situ polycondensation of P17-E in the presence of Bi_2MoO_6 nanobelts and microspheres, respectively.

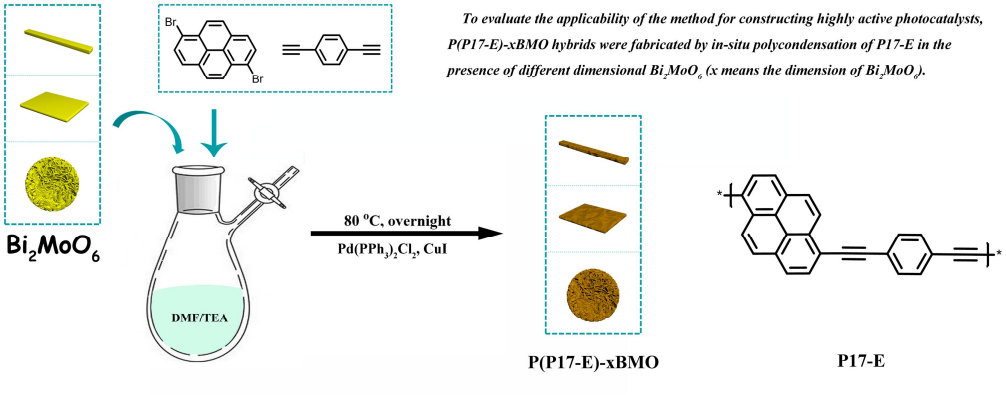

Scheme S1. In situ generation of P17-E on the surface of different dimensional Bi_2MoO_6.

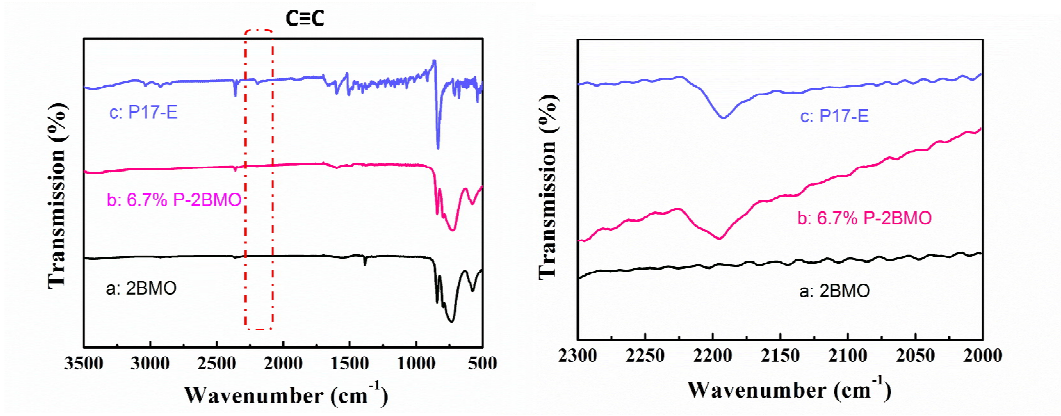

Figure S1. FT-IR spectra of 2BMO, 6.7% P-2BMO and P17-E.

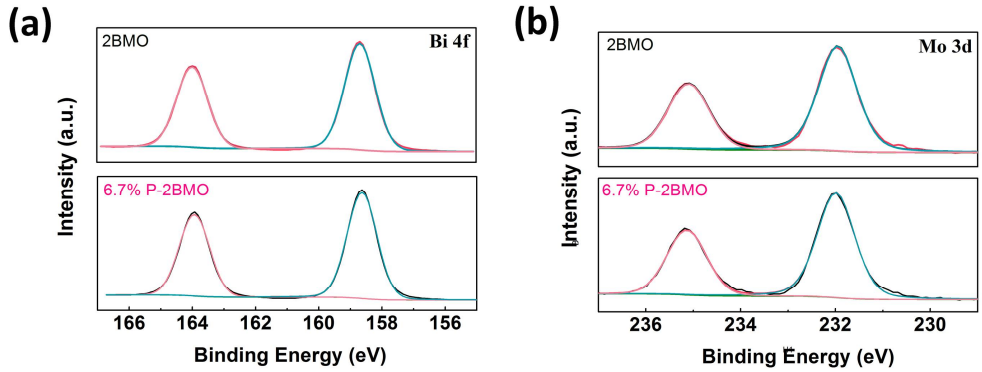

Figure S2. (**a**) XPS spectra of Bi 4f (**b**) and Mo 3d.

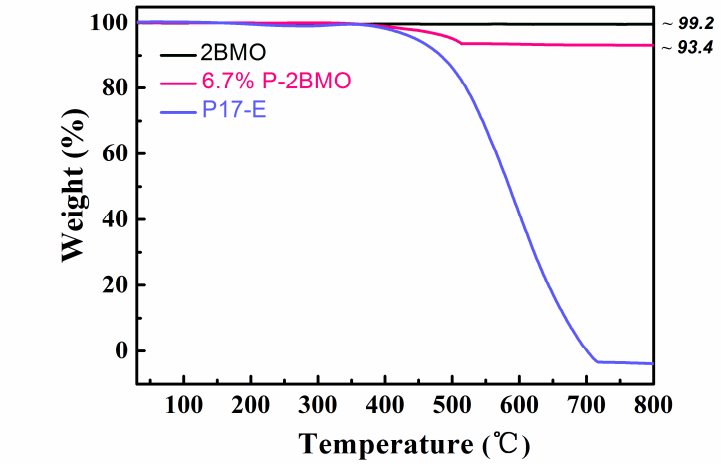

Figure S3. TG analysis of 2BMO, 6.7% P-2BMO and P17-E.

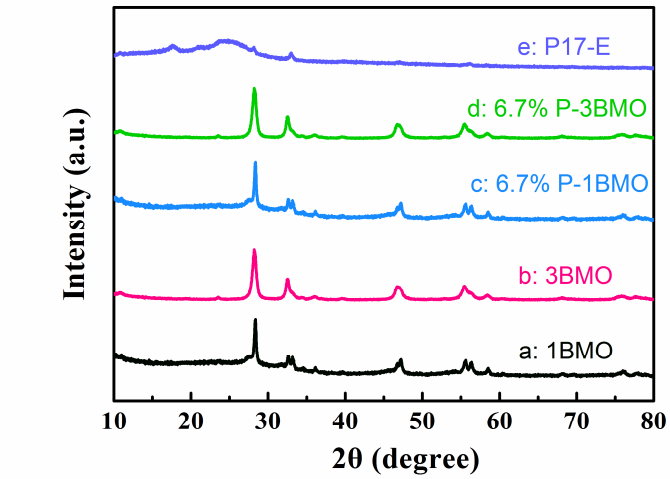

Figure S4. XRD patterns of 1BMO, 3BMO, 6.7% P-1BMO, 6.7% P-3BMO and P17-E.

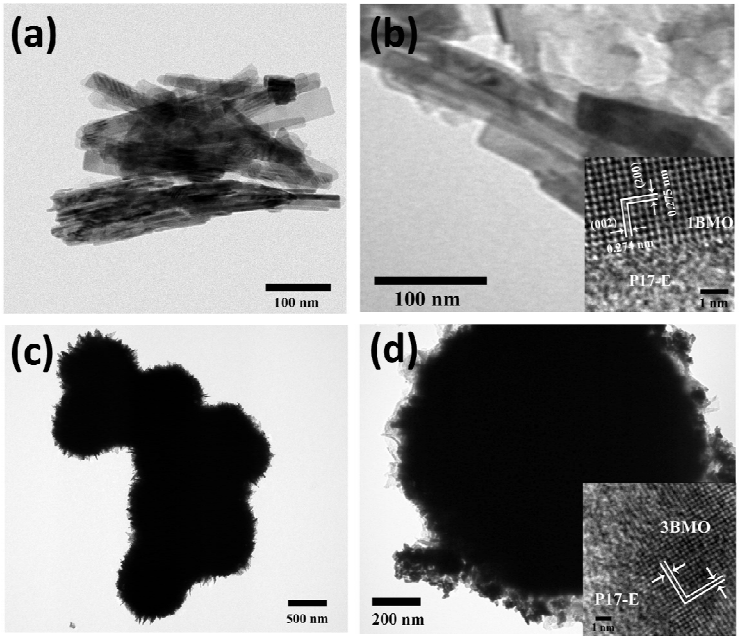

Figure S5. TEM images of 1BMO (**a**), 6.7% P-1BMO (**b**), 3BMO (**c**) and 6.7% P-3BMO (**d**), inset shows the corresponding HRTEM images.

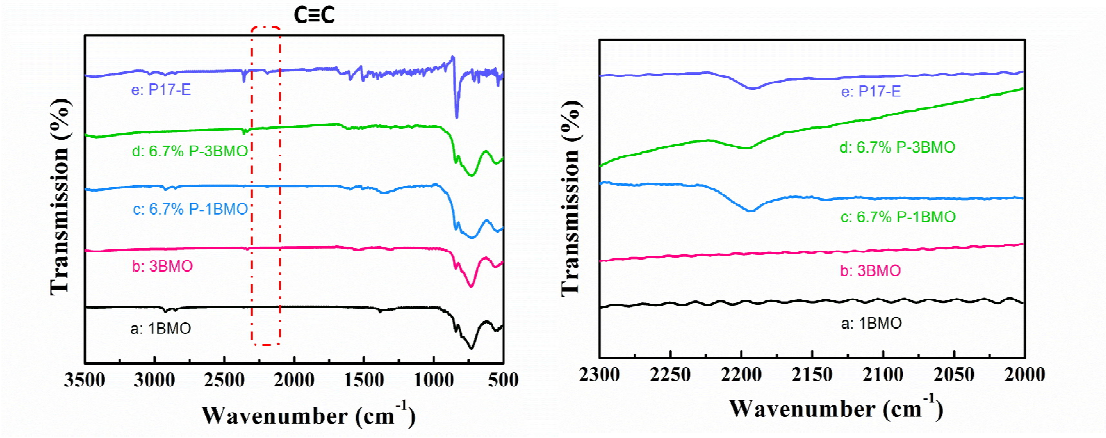

Figure S6. FT-IR spectra of 1BMO, 3BMO, 6.7% P-1BMO, 6.7% P-3BMO and P17-E.

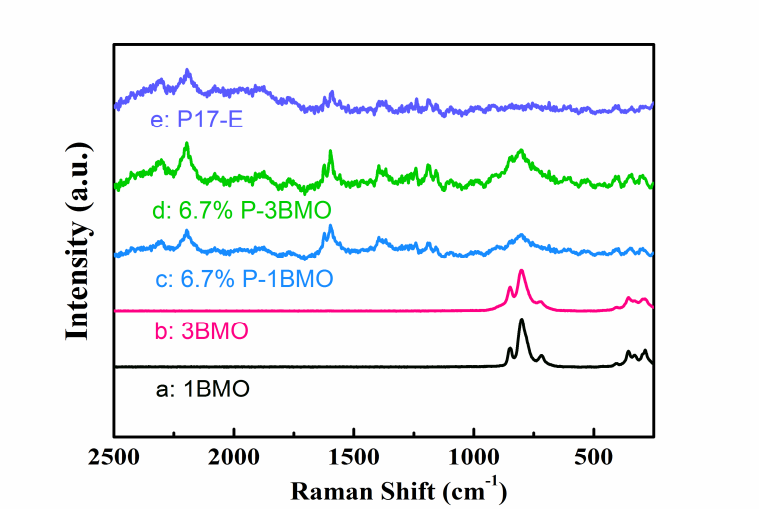

Figure S7. Raman spectra of 1BMO, 3BMO, 6.7% P-1BMO, 6.7% P-3BMO and P17-E.

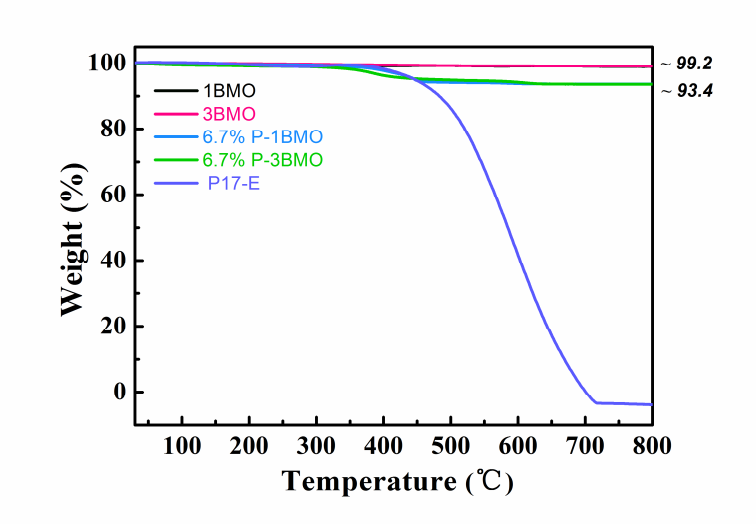

Figure S8. TG analysis of 1BMO, 3BMO, 6.7% P-1BMO, 6.7% P-3BMO and P17-E.

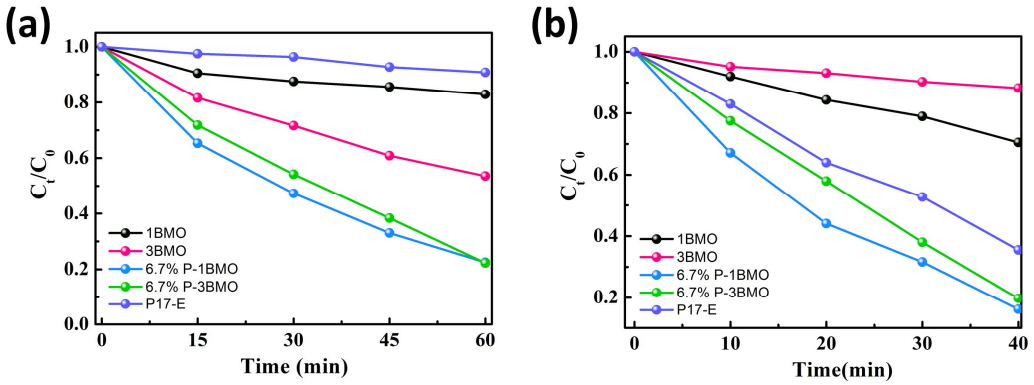

Figure S9. Photodegradation of ciprofloxacin (**a**) and photoreduction of Cr(VI) (**b**) over 1BMO, 3BMO, 6.7% P-1BMO, 6.7% P-3BMO and P17-E.

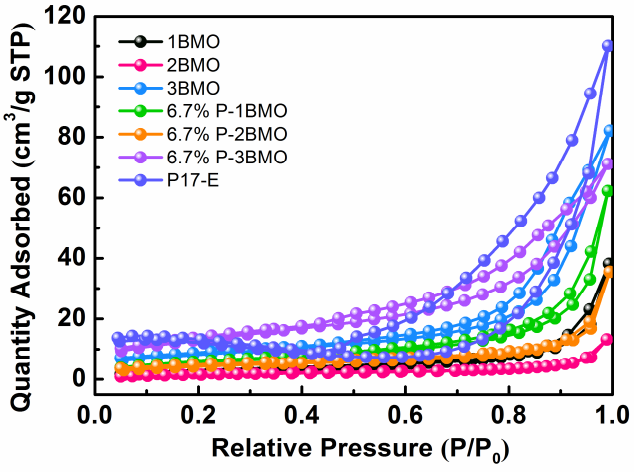

Figure S10. N_2-adsorption-desorption isotherms of all the samples.

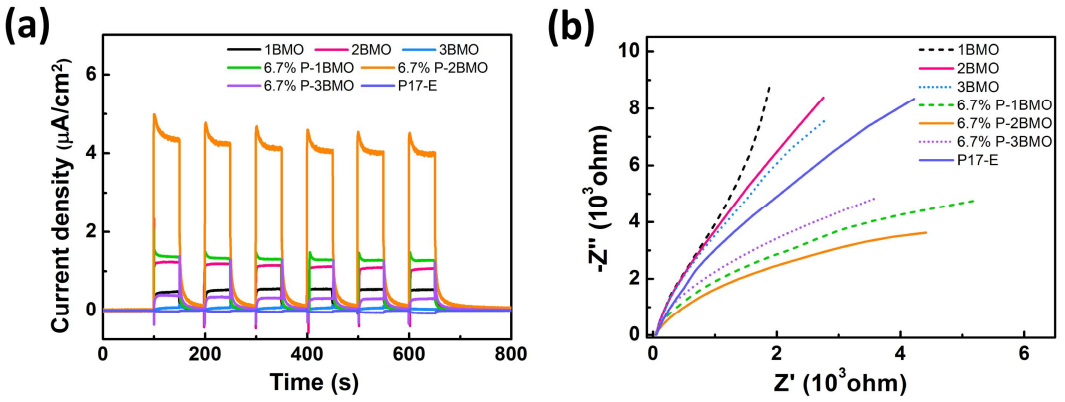

Figure S11. Photocurrent response spectra (**a**) and electrochemical impedance spectra (**b**) of all the samples.

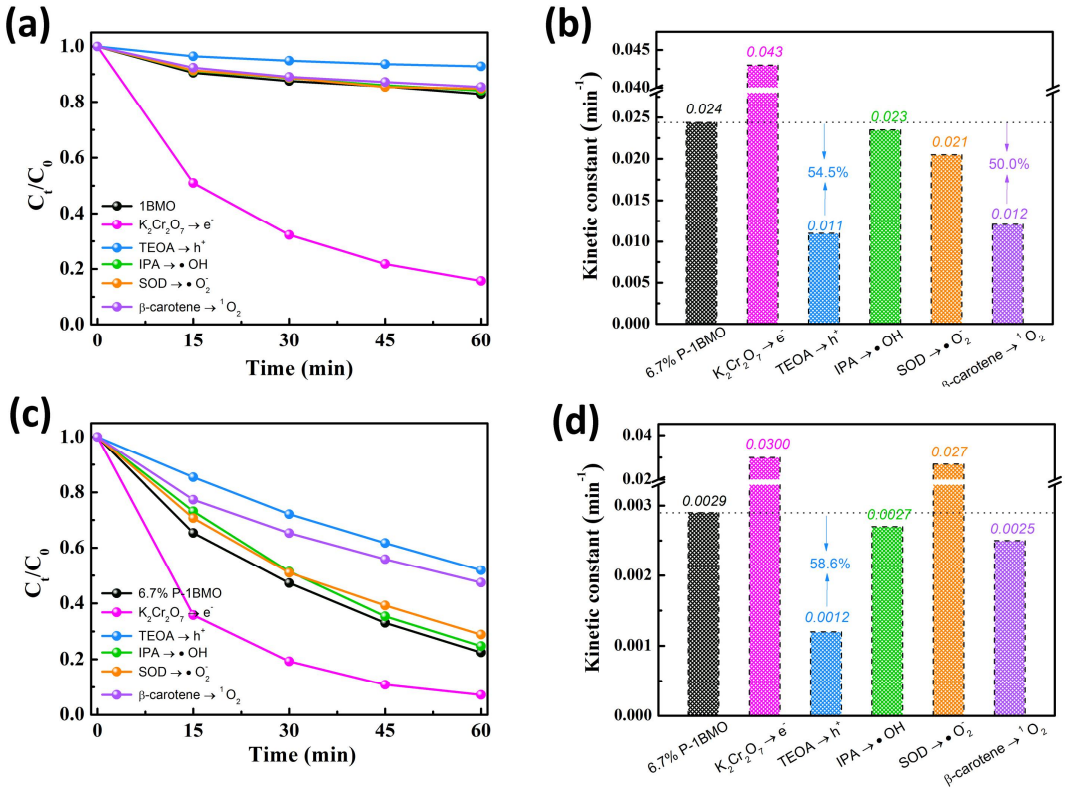

Figure S12. Trapping measurements and the corresponding rate constants for ciprofloxacin photodegradation over 1BMO (**a**, **b**) and 6.7% P-1BMO (**c**, **d**).

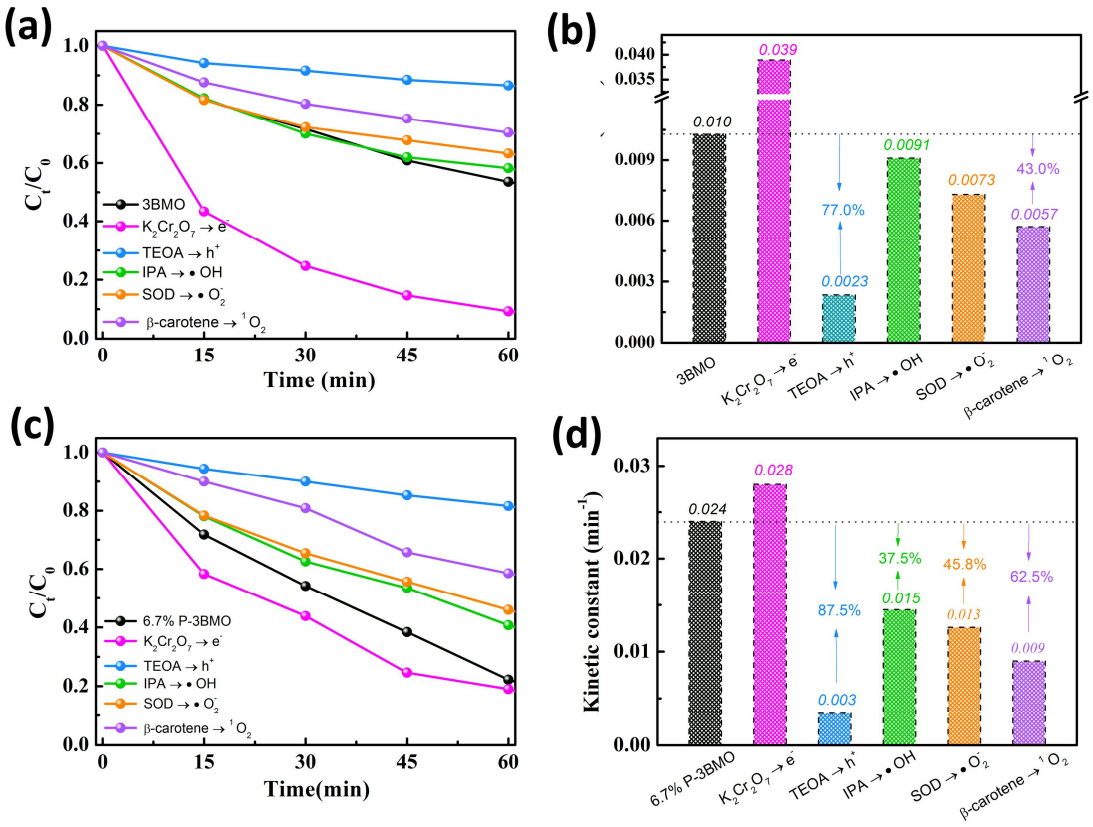

Figure S13. Trapping measurements and the corresponding rate constants for ciprofloxacin photodegradation over 3BMO (**a**, **b**) and 6.7% P-3BMO (**c**, **d**).

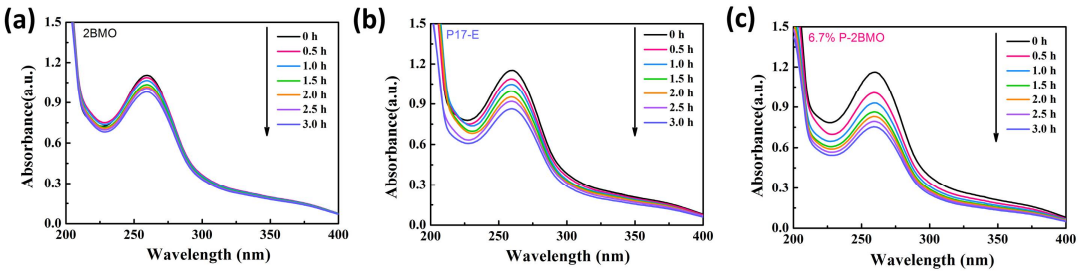

Figure S14. Spectra of NBT transformation generated by 2BMO (**a**), P17-E (**b**) and 6.7% P-2BMO (**c**) under visible light irradiation.

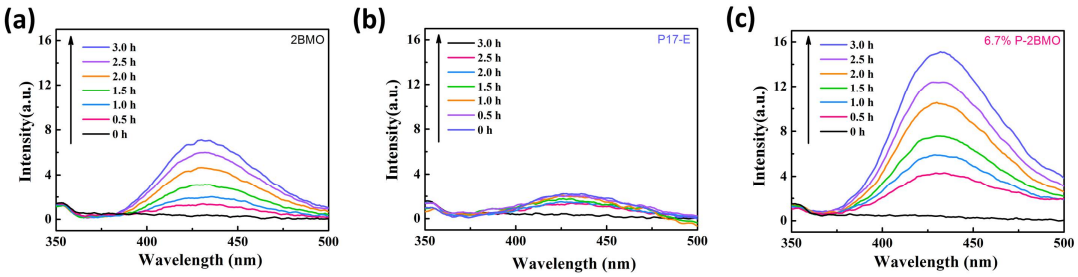

Figure S15. Fluorescence intensity of •OH-trapping PL spectra of 2BMO (**a**), P17-E (**b**) and 6.7% P-2BMO (**c**) under visible light irradiation.

Table S1 BET surface areas of all the samples.

Sample	1BMO	2BMO	3BMO	6.7% P-1BMO	6.7% P-2BMO	6.7% P-3BMO	P17-E
BET surface (m^2/g)	11.6	6.80	29.2	21.1	15.6	47.3	30.4
Normalized rate (10^{-4} g min^{-1} m^{-2})	2.50	12.9	3.42	11.4	21.8	5.07	0.658

Table S2 The analysis of band positions for 1BMO, 2BMO and 3BMO.

Sample	E_f vs. Ag/AgCl (V, pH=7)	E_f vs. NHE (V, pH=0)	VB vs. NHE (V, pH=0)	E_g (eV)	CB vs. NHE (V, pH=0)
1BMO	-0.92	-0.31	-0.41	2.61	2.20
2BMO	-0.87	-0.26	-0.36	2.62	2.26
3BMO	-0.85	-0.24	-0.34	2.63	2.29

References

1. Long, J.; Wang, S.; Chang, H.; Zhao, B.; Liu, B.; Zhou, Y.; Wei, W.; Wang, X.; Huang, L.; Huang, W. Bi_2MoO_6 nanobelts for crystal facet-enhanced photocatalysis. *Small* 2014, *10*, 2791-2795.